



# The assessment of a method for measurements and lead quantification in air particulate matter using total reflection X-ray fluorescence spectrometers<sup>☆</sup>



Laura Borgese<sup>a,b,\*</sup>, Fabjola Bilo<sup>a,b</sup>, Annalisa Zacco<sup>a,b</sup>, Stefania Federici<sup>a</sup>, Anne Wambui Mutahi<sup>a</sup>, Elza Bontempi<sup>a,b</sup>, Krystyna Trzepla<sup>c</sup>, Nicole Hyslop<sup>c</sup>, Sinan Yatkin<sup>c</sup>, Peter Wobrauschek<sup>d</sup>, Joseph Probst<sup>d</sup>, Dieter Ingerle<sup>d</sup>, Laura E. Depero<sup>a,b</sup>

<sup>a</sup> INSTM and Chemistry for Technologies Laboratory, Department of Mechanical and Industrial Engineering, University of Brescia, Via Branze 38, 25123, Italy

<sup>b</sup> SMART SOLUTIONS srl, Via Corfù 106, 25124 Brescia, Italy

<sup>c</sup> Air Quality Research Center, University of California Davis, One Shields Ave., Davis, Ca 95616, USA

<sup>d</sup> TU Wien Atominstitut, Stadionallee 2, 1020, Austria

## ARTICLE INFO

### Keywords:

Pb  
Filter  
Particulate matter  
GIXRF  
TXRF

## ABSTRACT

This paper presents the assessment of a direct method to measure and analyse Pb in air particulate matter (PM) collected on polytetrafluoroethylene (PTFE) filtering membranes prepared by the SMART STORE<sup>®</sup> procedure. The suitability of grazing incidence X-ray fluorescence technique is verified on a set of continuous and conformal thin film samples created by atomic layer deposition. Different scans changing the angles of incidence are performed and the fluorescence intensity of thin films on PTFE substrate compared with that obtained by similar thin films deposited on Si wafer substrates. The effects of sample preparation, constraints, and limitations of the experimental setup are discussed. The results obtained by three commercial total reflection X-ray fluorescence spectrometers, equipped with Mo or Rh X-ray tubes, are compared. Reference samples with different Pb content are used to define the best measurement conditions, corresponding to the maximum fluorescence intensity. The precision is evaluated in terms of relative standard deviation of the net intensity, taking into account the homogeneity of the PM samples and hardware contributions to the errors. The calibration curves are built on the basis of mono- and multi-elemental Pb loaded PTFE reference samples. The analytical parameters, namely linear calibration and determination range, limits of detection, and quantification, are determined.

## 1. Introduction

Particulate matter (PM) is a prominent pollutant in the air, produced by human activity and natural phenomena [1]. PM morphology and chemical composition are strongly dependent on their origin [2]. Common elements in PM are aluminum, calcium, iron, magnesium, potassium, and silicon, usually present in their oxidized states. Other potentially toxic elements, such as cadmium, arsenic, chromium, lead, and nickel may also be present [3,4].

PM causes respiratory, cardiovascular [5,6], and other diseases, mainly depending on their particle size: PM with aerodynamic diameters less than 10  $\mu\text{m}$  ( $\text{PM}_{10}$ ) is eliminated by the inhalation system while PM with aerodynamic diameters less than 2.5  $\mu\text{m}$  ( $\text{PM}_{2.5}$ ) enters the lung alveoli and can get into the bloodstream [5,7,8]. In view of the

strong interaction of PM with human health, it is important to determine the chemical composition and identify their origins [9].

The reliability and accuracy of air sampling methods depend on many factors including the concentration levels and particle size of interest. Many methods and instruments are proposed, based on specific PM physical properties, collection medium type, airflow rates, and sampling efficiency [10–13]. The filtering media, more commonly called filter, is the most important element in PM sampling, and gravimetric filter analysis remains the reference method since the filters have proven to be a reliable medium for trapping the PM [2,14–18]. Three main kinds of commercial filters are used to evaluate specific characteristics of the particles: fibrous, porous, and capillary pore membrane filters. The collection efficiency, the pressure drop during sampling, and the analytical method employed after sampling

<sup>☆</sup> Selected Paper from the 18th International Conference on Total Reflection X-Ray Fluorescence Analysis and Related Methods (TXRF 2019) held in Girona (Spain), June 25–28, 2019

\* Corresponding author at: INSTM and Chemistry for Technologies Laboratory, Department of Mechanical and Industrial Engineering, University of Brescia, Via Branze 38, 25123, Italy.

E-mail address: [laura.borgese@unibs.it](mailto:laura.borgese@unibs.it) (L. Borgese).

<https://doi.org/10.1016/j.sab.2020.105840>

Received 15 November 2019; Received in revised form 12 February 2020; Accepted 24 March 2020

Available online 26 March 2020

0584-8547/ © 2020 Elsevier B.V. All rights reserved.

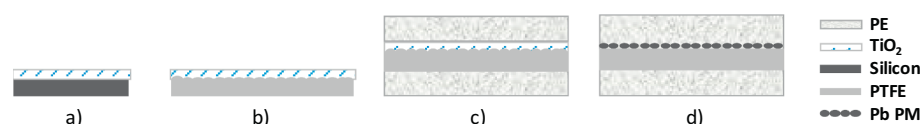


**Fig. 1.** Schematic cross section view of the samples a) Ti/Si, b) Ti/PTFE before and c) after the SMART STORE<sup>®</sup> procedure, and d) Pb series. Proportions are not respected.

determine the proper filter to be used [19]. The European norm EN 12341 “Air quality – Determination of the PM<sub>10</sub> fraction of suspended particulate matter – Reference method and field test procedure to demonstrate reference equivalence of measurement methods” (1999) [20], defines the principle method for PM<sub>10</sub> analysis as sampling particulate matter on a filter. When elemental analysis must be performed, the suitable filters are: Acetate Cellulose Filters, polytetrafluoroethylene (PTFE), Polycarbonate, Borosilicate and quartz filters. PTFE filters are usually preferred since they have lower impurities than quartz and a smoother surface.

The chemical analysis of PM can be performed using sensitive wet chemistry based methods such as Atomic Absorption Spectroscopy (AAS) [21], inductively coupled plasma-optical emission spectroscopy (ICP-OES), and mass spectrometry (ICP-MS), ion chromatography and voltammetry. Reference analytical methods for heavy metals analysis of PM filter samples, established by European Directive [22,23], are Graphite furnace-AAS and ICP-MS. Today, ICP-Atomic Emission Spectroscopy (AES) and ICP-MS have become the principal analytical tools to determine trace elements in PM [24]. The main drawback of these techniques is the preparation procedure, which is time consuming, expensive, and environmentally unsustainable, since it is based on acid digestion. Problems associated with the determination of trace elements in airborne PM samples using microwave digestion method have already been discussed [25].

X-ray based techniques overcome these disadvantages since sample digestion is not necessary and are considered suitable for PM analysis on PTFE filters [26,27]. Recently, XRF spectrometry techniques have become more common in multi elemental analysis [28]. Indeed, ED-XRF is recognized as a proper technique for the determination of metals and metalloids for ambient atmospheric PM filter samples by the United States Environmental Protection Agency (EPA) [29].

Quantitative chemical analysis by XRF is achieved using standard samples with known concentrations: the calibration procedure is based on the relationship between elemental mass and the intensity of the element fluorescence lines assuming a constant matrix effect [30]. The volume/spatial homogeneity of the sample and the stability of the signal are fundamental to obtain reliable analytical results. Additional methods have been proposed to correct for instrumental drift inter-element interferences and matrix effects [30]. A simplified calibration procedure, known as “empirical”, directly compares the net intensity of the element fluorescence line with the concentration of the standard sample, assuming a constant matrix calibration factor. This “empirical” approach can be used when the sample in analysis and the standard sample matrix compositions are similar. Typically, direct analysis of aerosol samples has been performed by EDXRF, which establishes a relationship between X-ray intensities and a number of calibration standard samples. However, there are still some disadvantages mainly due to the lack of appropriate reference standards for quantitative analysis calibration method [31–33].

In more recent years, total reflection XRF (TXRF) spectrometers have also been used to analyse PM filter samples using various sample preparation procedures [28]. TXRF is a technique for the surface chemical analysis exploited in many application fields to measure low sample volumes on reflective surfaces [34–36]. This technique has multiple advantages, such as the simple calibration and low detection limits for many elements [37]. The assumption of the method is that the sample must be a thin film on a flat substrate. Development and commercialization of benchtop TXRF instrumentation have promoted its application in many environmental fields including the analysis of

water [34,38–40], biomonitors [41–43], plants [44–46], biological samples [13,47,48], cosmetic [49,50], pharmaceutical and drug [51–53] and food [54–56]. Attempts have been made to achieve direct sampling of PM on quartz reflectors [57], but the possibility of PM bounce effects and the lack of specific standards for such sampling lead to low representativeness of this collection method with respect to filters.

Previous studies have shown how TXRF instrumentation can be employed to evaluate the elemental composition of PM on PTFE filters [6,58] and tree leaves [41], successfully addressing contamination and sample thickness issues by sandwiching the sample between two thin polymeric sheets, cutting the plastic ring stretching the PTFE, and placing the sample on a TXRF carrier for the analysis. This sample preparation procedure, called SMART STORE<sup>®</sup>, was developed in 2008 to measure PM filter samples by a commercial TXRF instrument to avoid possible detector damages. The benefits of sample protection and storage, and the suitability of SMART STORE<sup>®</sup> for the qualitative analysis based on X-Ray techniques have previously been discussed [59]. However, the quantitative analysis has some difficulties, related to the experimental setup and analysis.

The PM filter samples are complex samples that can be described as a smooth surface covered by particles with different sizes, shapes, and chemical compositions (see Fig. 1c). The PM deposition on the filter surface is assumed to be spatially homogeneous, and that assumption mainly depends on the sampling device. Previous works showed that the behavior of filters prepared by the SMART STORE<sup>®</sup> procedure may be modeled with a high degree of accuracy as thin-film-like [58].

The main aim of this work is to assess the SMART STORE<sup>®</sup> procedure to perform quantitative elemental analysis of the Pb content in PM filter samples using a TXRF spectrometer with variable incidence angle, the empirical calibration approach, and a set of novel reference standards. To demonstrate the reliability of this method, it has been applied to a set of model samples created by Atomic Layer Deposition of TiO<sub>2</sub> thin films with a thickness of about 1 nm on silicon wafer and PTFE membrane substrates. An in-depth evaluation is discussed in this paper.

## 2. Material and methods

### 2.1. Samples

The samples analysed in this study are summarized in Table 1. The calibration curve was built using Pb loaded mono- and multi-element reference samples of PM on 2 μm pore size 47 mm diameter PTFE membranes, provided by Air Quality Research Center at University of California, Davis (AQRC-UCD) [26,33]. The mono-Pb samples were generated using lead acetate trihydrate salt (99.999% purity, Sigma-

**Table 1**  
Summary of the analysed samples, substrate material and respective elemental loading, reference to the kind of sample type presented in Fig. 1 is also given.

Name	Substrate material	Element loading (μg/cm <sup>2</sup> )	Sample type
Blank	PTFE	0	d)
Pb_ME	PTFE	0.028	d)
Pb1	PTFE	0.594	d)
Pb2	PTFE	0.69	d)
Pb3	PTFE	4.239	d)
Pb4	PTFE	10.169	d)
Ti/Si	Si wafer	0.137	a)
Ti/PTFE	PTFE	0.137	b) and c)

Aldrich, St. Louis, MO, USA) solution prepared in ultrapure water (Type 1 water, Milli-Q, Billerica, MA, USA). The solution was then introduced to a custom-made aerosol deposition system (AGS) [31,33]. The solution was atomized, dried and collected on PTFE filters. Before and after deposition, the filters were dried in a desiccator for 48 h followed by gravimetric measurements utilizing an ultrabalance (Mettler XP2U, Switzerland, 0.1  $\mu\text{g}$  sensitivity) on three different days. Before weighing, the filters were placed on polonium strips in room temperature/humidity to eliminate the static as well as to equilibrate them with room air. Quality assurance/control measures including calibration, verification of calibration by certified weights and weighing of test filters were applied prior to each weighing. The Pb-loadings were calculated using the net deposit mass, deposition area, and the purity and stoichiometry of lead acetate. The Pb-loadings were also confirmed by XRF analyses at UCD AQR. Multi-element Pb samples were generated from certified multi-element solutions (High Purity Standards, NC, USA) using AGS [31]. The Pb-loadings were determined using an approach based on two assumptions, being the XRF potassium measurement at UCD-AQR is accurate and the elemental ratios in the certified solutions are preserved on the generated multi-element Pb samples. These assumptions were verified by internal and external measurements [31,32]. A Pb loading around 0.415  $\mu\text{g}/\text{cm}^2$  is expected on a 47 mm diameter filter measured for 24 h at 10 L/min at the 0.5  $\mu\text{g}/\text{m}^3$  Pb concentration limit value of the EU Directive [33]. For this reason, the sample Pb1 having a Pb loading just above the limit was considered for extensive characterization.

Compact and uniform thin film  $\text{TiO}_2$  samples were prepared by means of the Atomic Layer Deposition (ALD) method with silicon (Si) wafer and 2  $\mu\text{m}$  pore size 37 mm PTFE membranes as substrates [58]. Concurrent deposition on Si and PTFE substrates was performed to guarantee the same thickness of the deposited  $\text{TiO}_2$  layer. Eight ALD cycles were performed resulting in an estimated layer thickness of about 0.54 nm, calculated on the basis of the growth rate calibration curve and a  $\text{TiO}_2$  density of 4.2  $\text{g}/\text{cm}^3$  [60–63].

The SMART STORE® sample preparation device was used to sandwich PTFE membranes between two sheets of laminated polyethylene and remove the PTFE stretching plastic. Fig. 1 shows a schematic cross section of the samples to highlight the different features of ALD thin films and PM on the two substrates. This procedure is mandatory for measuring filter samples with a stretching plastic ring to keep the membrane flat. Indeed, the ring thickness impedes the irradiation of the surface where PM is collected and it must be removed prior measurements. Without the ring and the plastic the sample is damaged by shrinking.

## 2.2. Measurements

Three TXRF spectrometers having different instrumental setups were used: the commercial S2 Picofox (Bruker); the Explorer prototype (GNR); and the custom made Wobicompact (Atominstut). The main differences among them are the incidence angle and the excitation source/energy.

S2 Picofox is equipped with a Mo X-ray tube and the incidence angle is set at  $0.07^\circ$  with respect to the surface identified by the three tips positioning system. Spectral analysis was performed by the instrument software (SPECTRA, Bruker). The complete experimental setup is reported in ref. [41].

The Explorer has a Mo X-ray tube, the incidence angle can be scanned with a step of  $\pm 0.0001^\circ$  and it is equipped with a goniometer. The complete configuration is described in ref. [58]. Before measuring the deposited substrates, angular scan of a blank Si wafer was performed to evaluate the position of the critical angle in the Si-K $\alpha$  intensity profile and determine the  $0^\circ$  value.

The Wobicompact is equipped with a Rh X-ray tube 50 W power (50 kV, 1 mA), a 150  $\text{mm}^2$  area silicon drift detector (SDD) (Ketec) and a CCD camera for beam alignment purposes and angle control. It allows

manual angular scan by screw rotation with height step width of  $\pm 10 \mu\text{m}$ . All the samples were placed on the surface of the same quartz glass reflector to maintain the aligning position and excited for 600 s or 300 s.

The Explorer and Wobicompact spectra collection software were set to give automatically the counts of the selected region of interest (ROI) without subtracting the background. Further spectral analysis was performed by PyMca software.

## 3. Results and discussion

A sandwiched filter having a total thickness about 350  $\mu\text{m}$  doesn't fulfill the ideal conditions of total reflection of X-Rays on the quartz reflector surface [6,41,58]. Thus, the proposed method is more properly named Grazing Incidence XRF (GIXRF), even though TXRF spectrometers are used to [59] provide an enhancement of the signal compared to the intensity obtained by the conventional XRF geometry (incidence angle about  $45^\circ$ ). However, for a quantitative analysis, issues arise related to both the samples and the measurement system. The PM deposit - homogeneity of deposit on the filter, PM size, PM composition, matrix effects all must be considered for the samples. - For the measurement system, the spectrometer geometry and measurements conditions affect the intensity absolute values, depending on the degrees of freedom and repeatability.

Sample dependent effects can be checked and often compensated for. As an example, a stabilization time is required before collecting repeatable measurements in the Picofox (see Fig. 2) without removing it from the measuring position. The fluorescence intensity of Pb L lines with respect to time is shown in Fig. 2 where the two curves correspond to two sample positions in the chamber. Experimental trials show that stabilization time around one hour is needed to get repeatable spectra. After 15 min the intensity changed more than 25% and in the following 45 min there is an additional change of about 15–20%. This effect probably results from the soft surface of the polymeric material coating the sample settling into the three positioning tips used to mount the sample in the analysis chamber. The polymeric material covering both sides of the membrane is soft and depression marks appear on the measured sample, suggesting a change in the sample position. This slight change in position may result in a different incidence angle as well as change in the irradiated sample area and, thus, a change in the fluorescence intensity clearly shown by the intensity difference at the plateau. (See Fig. 3.)

Variability is observed also measuring the same sample after the gradual settling resulting in a RSD of about 16% in the net area of Pb L lines. These results show the difficulty of accurately determining elemental content using this experimental setup. Thus, a proper measurement procedure must be developed starting from the assumptions and basis of GIXRF.

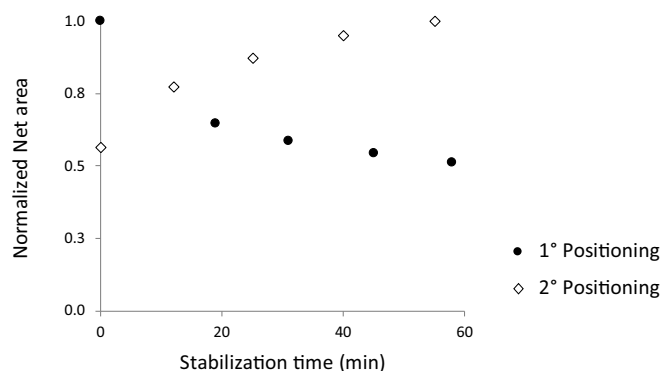


Fig. 2. Net area of Pb L lines of sample Pb1 as a function of the stabilization time normalized to the maximum. The two datasets correspond to different sample positioning in the S2 Picofox measuring chamber.

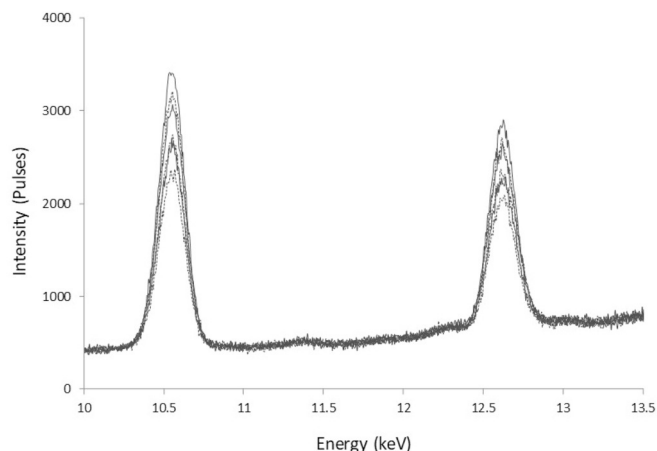


Fig. 3. Spectra of sample Pb1 in the energy range of Pb L lines, measured six times after repositioning in the S2 Picofox.

The fluorescence intensity of Ti K $\alpha$  ROI was measured on TiO<sub>2</sub> thin film model samples with Explorer varying the incident angle, as shown in Fig. 4. The fluorescence signal of Ti on Si and PTFE substrates show the intensity profile usually modeled either as granular residue and/or a thin film on a thick substrate, so called thin-film-like profile [58], with a maximum at the critical angle of incidence of the substrate, due to the presence of a standing wave field on the surface. The angular position of the maximum in both the experimental curves is slightly higher than that calculated for Si and PTFE, from the tabulated refraction indexes, 0.099° and 0.134° respectively. The shift is about 0.02° for Si substrate and is of 0.10° for the membrane, as it may be expected [64,65]. Peak broadening observed with PTFE substrates was modeled as an effect of the beam divergence [58], and it may also be due to surface roughness, higher in case of PTFE. Intensity oscillations are observed for both substrates, probably due to interference effects with the reflecting TiO<sub>2</sub> layer, having calculated critical angle about 0.097°. This feature is more evident on PTFE due to its with regular patterns [58]. The higher fluorescence intensity detected on the filter substrate can be ascribed to the larger surface analysed and thus the larger Ti amount.

As it is expected due to absorption effects, the SMART STORE® procedure decreases the fluorescence intensity of the sample due to the presence of plastic. The angular scan merges the features of the previously observed PTFE curve with one additional thin-film-like profile, with a local maximum at 0.1°. This intensity increase is compatible with the presence of a standing wave on the polyethylene (PE) surface. The

PE has calculated critical angle of 0.07°, and the local maximum occurs with a right shift previously observed. The sharp features observed in the region 0.1°–0.15° are maybe due to an interference of the two profiles. On this basis, the angular response of the fluorescence intensity should be carefully considered in the case of a quantitative analysis without internal standard. In addition, the angle of incidence must be set at the maximum of the intensity to exploit the enhancement effect of the grazing incidence measurements.

The model samples of membrane covered by a continuous ideal thin film may not be representative of the actual PM filter samples, characterized by PM of various shapes and sizes deposited on smooth PTFE filters. For this reason, further experiments were performed with novel reference materials for PM filter samples [31]. Pb loaded samples were selected due to the interest in Pb determination for environmental reasons. The measurements of Pb loaded reference samples were performed with the Wobicompact spectrometer, which can set manually the incidence angle of X-Ray beam, rotating the disc reflector along its surface center. The beam size cut at about 500  $\mu$ m width enables to measure sections of the samples. The intensity of Pb L alpha ROI (10.28–10.71 keV) is measured as a function of the incidence angle for the sample Pb1 at fixed position in the spectrometer without removing it from the quartz carrier. Both the incoming and reflected beam were observed before the maximum of the curve, suggesting a high degree of beam reflection. The expected thin-film-like profile is observed and compared with that of a real thin film sample, the Ti/PTFE plasticized sample (see Fig. 5). For comparison, normalized intensities are displayed on the ordinate axis and a geometrical conversion factor is used for the abscissa axis. The ratio between the screw displacement position and its value at the maximum, assumed as the critical angle position, is used as independent variable for the Wobicompact measurements. Differently, the ratio between the sine of the incidence angle and the sine of the critical angle is considered for Explorer measurements. The two patterns show the same peak broadening, while being quite different, as it may be foreseen because of the different instrumental configuration and excitation sources. It is worth notice that both samples show an enhancement of the signal around the critical angle, although they are very different, being made respectively by a nanometric thin film (modeled as type c) and particles with variable size (modeled as type d). This was somehow unexpected from a theoretical point of view, but we already observed it consistently in many experimental studies, and it may be due to the presence of a standing wave. The angular response of PM loaded filters gives the main justification to the assessment of the proposed measurement method involving the determination of the condition to achieve the maximum intensity

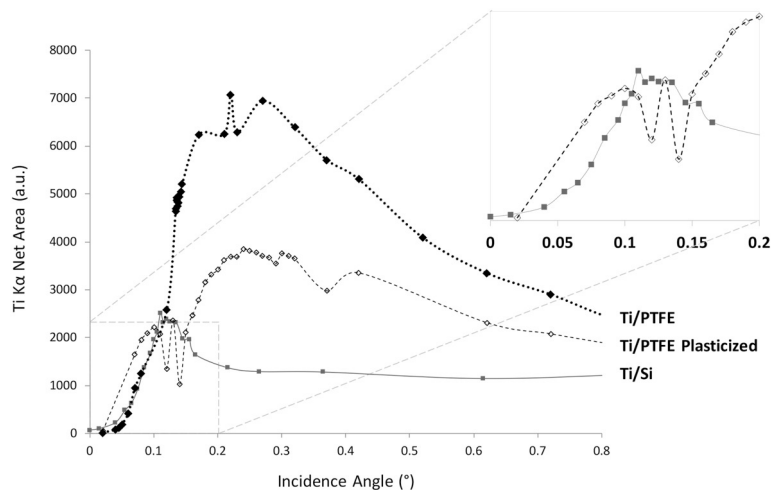


Fig. 4. Ti K $\alpha$  intensity profiles of TiO<sub>2</sub> thin films deposited on Si (Ti/Si) and PTFE (Ti/PTFE) substrate before and after (Ti/PTFE Plasticized) the SMART STORE® procedure. The inset shows a magnification of the lower angle range up to 0.2°.

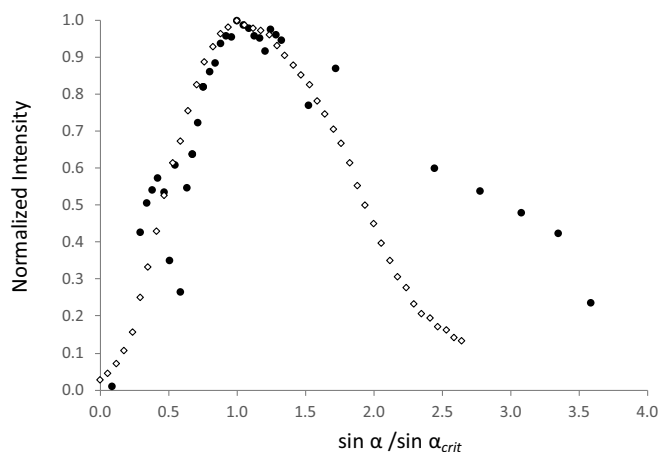


Fig. 5. Comparison of the normalized intensity of Pb  $\alpha$  and Ti  $\alpha$  ROIs collected as a function of the incidence angle with Wobiccompact on sample Pb1 (squares) and Explorer on plasticized Ti/PTFE (circles).

before proceeding with the calibration.

Fluorescence intensities are one order of magnitude higher for Pb (see Fig. 6) in agreement with the higher loading. The sum of the two thin film profiles of PE and PTFE are not visible, confirming the loss of the thin film structure. This profile is expected for any sample having the same substrate measured on the top of a quartz carrier.

In sample Pb1, Pb is detected in all the experimental conditions, thus showing the suitability of GIXRF for analyzing Pb in air filters for environmental monitoring. The fluorescence intensity of Pb L alpha changes about one order of magnitude in the angle scan and the incidence angle of the maximum is selected for quantitative analysis, with the same approach used for the validation of the method for TXRF analysis of water [34].

Precision is evaluated by repeating measurements at least three times to check the repeatability of the four conditions described below. The relative standard deviation (RSD %) of the net peak area for each set of measurements is reported in Table 2.

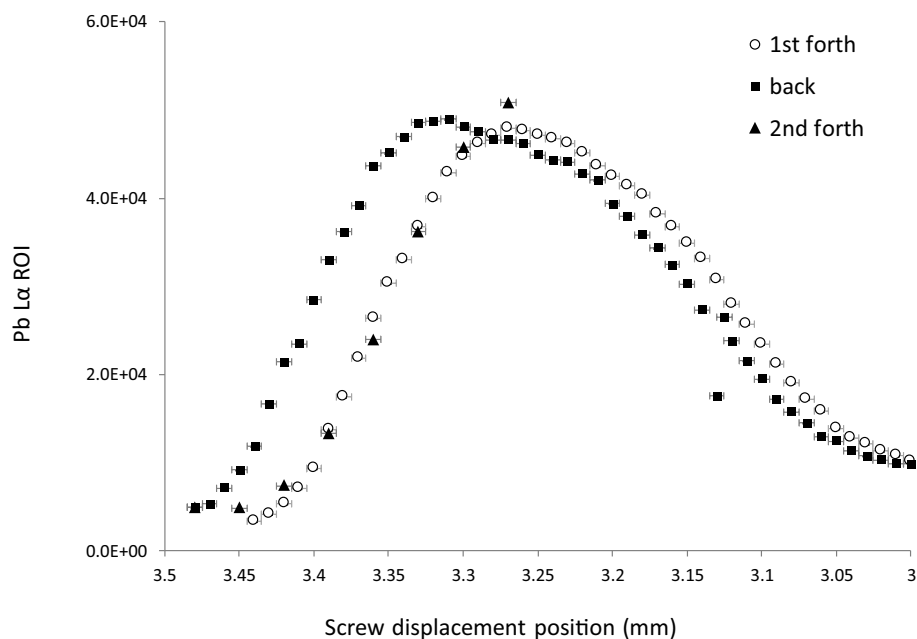


Fig. 6. Angular scan curves of Pb  $\alpha$  ROI collected on sample Pb1 with Wobiccompact increasing (circles) and decreasing (squares) the incidence angle back and forth to check repeatability of angle positioning at the maximum.

Table 2

Repeatability expressed as fluorescence intensity RSD % of the set of measurements performed to test (i) the counting statistics; (ii) the height positioning, (iii) sample homogeneity, and (iv) the angle positioning at the maximum. In the case of sample homogeneity specification of single operator (S) and multiple operators (M) is given.

Repeatability	RSD %
(i) Counting statistics	0.2
(ii) Height positioning	1.2
(iii) Sample homogeneity (rotation + height)	4.7 (S) 5.4 (M)
(iv) angle positioning at the maximum	3.3

- (i) the counting statistics of the selected ROI without moving the sample from the spectrometer chamber; the sample is not moved from its position in the spectrometer chamber and the area of the selected ROI is calculated for 5 sequential measurements to evaluate counting statistics uncertainty.
- (ii) the height positioning (by taking the sample in and out); the calculated RSD is acceptable considering that a background curve is not included. Sample positioning in the Wobiccompact is done manually by rotating an eccentric drive, a device component acting on the lifter with the reflector on top that brings up the reflector from the insertion position to the position for measurements. The most critical issue is the lack of a height limit tool/system to achieve the same position, which would avoid the user-dependent repositioning. RSD on 5 repetitions is, again, well below the acceptable 10%.
- (iii) sample homogeneity (by rotating the sample about 45° on its center); it cannot be tested separately from the contribution of height position, as the filter must be rotated by removing it from the measuring chamber. RSD is calculated on 5 repeated measurements by the same operator plus 8 measurements made by two additional operators. This uncertainty is the highest and may be considered the sum of all the previous contributions.
- (iv) the angle positioning at the maximum by repeating the angle scan back and forth. The angle scan is repeated three times rotating the displacement screw clockwise and counterclockwise back and forth and the maximum intensity is recorded. The angular scan

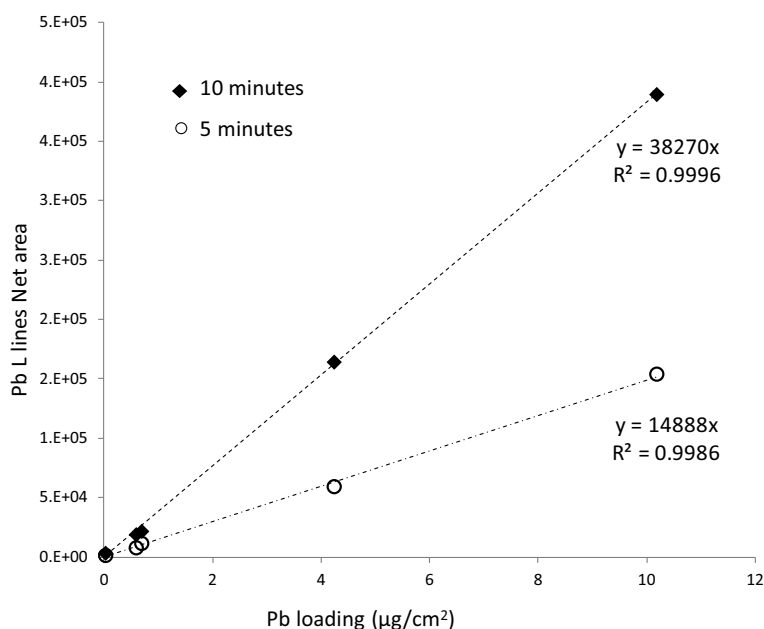


Fig. 7. Calibration curves experimental data and linear regression of the two datasets of measurements with 10 min (square) and 5 min (circles).

curves are superimposable increasing the incidence angle, while there is a slight shift observed when rotating in the opposite direction. However, the maximum intensity is not significantly different. It is worth notice that RSD is about one order of magnitude higher than that of counting statistics. This is expected from the shape of the curve and the sensitivity of the height positioning screw, about 5 µm. Improvements can be made by increasing the sensitivity of screw height positioning system.

The method for Pb analysis is assessed by measuring the set of Pb loaded reference samples (see Table 1) without changing the incidence angle with respect to the position of the maximum intensity of the angular scan curve used to build the calibration line. According to the EPA Guidelines EPA/625/R-96/010a [29], reference samples should have the same matrix, and thus Pb loaded PTFE membranes were selected. The calibration curves are built measuring the Pb loaded reference and the blank samples in the same experimental configuration. An additional set of measurements is repeated reducing lifetime from 10 to 5 min. Net areas of Pb L alpha lines are obtained from spectral analysis of each measurement by PyMCA and plotted against the quoted Pb loadings in Fig. 7. For each dataset linear regression is performed at the 95% confidence interval. In both cases the intercept is not significantly different from zero, based on the student *t*-test at the 95% probability. Thus, a new linear regression is performed setting the intercept to zero. Equations are reported in Fig. 7.

The significance of the linear regression model is very high over the whole concentration range, as it is highlighted by the coefficients of determination ( $R^2$ ) being higher than 0.99, and the F test values in the  $10^{-6}$  order of magnitude. The residuals plots have no trend and no further statistical evaluation of regression has been made. Clearly, there are no issues related to uncompensated matrix effects for higher loadings. A decrease of the performance due to the presence of other elements it is not expected considering that the results of sample Pb<sub>ME</sub>, having the lowest Pb loading, belong to the calibration line. Estimation of the limit of Blank (LOB), limit of detection (LOD) and quantification (LOQ) of Pb is performed according to the IUPAC method using the measurements of the blank and reported in Table 3. Only in the case of the “5 min life time” measurements the LOD is lower than the first level of the calibration curve. The acceptability criterion requests that LOD lays between half and one time the first concentration level of the

Table 3

Estimation LODs and LOQs of Pb according to the IUPAC method.

Measurements life time	LOB	LOD	LOQ	Determination range µg/cm <sup>2</sup>	Slope
10 min	0.044	0.048	0.069	0.594–10.169	38270 ± 304
5 min	0.010	0.011	0.020	0.028–10.169	14888 ± 219

determination range, and the Pb<sub>ME</sub> sample should be excluded from the “10 min” measurements dataset because the Pb concentration is below the LOD. Improvements of LoB, LODs and LOQs should be achieved by multiplying the number of measurements of the blank. This will allow to satisfy the requirements for possible environmental monitoring of Pb also for this measurement dataset.

#### 4. Conclusions

The assessment of a method for measurement and analysis of PM filter samples using three commercial TXRF spectrometers is presented. The most suitable experimental conditions to analyse PTFE filters prepared with the SMART STORE® are determined by applying the empirical calibration approach. It is shown that sample repositioning in the commercial TXRF spectrometer (S2 Picofox) with a fixed incidence angle configuration is the most critical parameter to achieve a reproducible and accurate measure.

The best experimental conditions were defined by studying the fluorescence intensity of Pb as a function of the incidence angle in model thin film samples and novel PM reference materials. The angular response of thin films is recorded in a Mo TXRF spectrometer (Explorer) equipped with a goniometer allowing automatic incidence angle set. As expected, the intensity profile strongly depends on the substrate and has a maximum at the critical angle. A significant peak broadening and enhancement effect is observed on PTFE substrate, confirming the thin-film-like behavior of PM filter samples.

The plastic sandwiching procedure named SMART STORE® introduces a second thin-film-like profile pattern attributable to reflection on laminated polyethylene. This effect, together with curve oscillations, is only observed in conformal thin film samples.

The angular response of a mono-elemental reference sample with Pb loading, being of environmental interest, is measured by a Rh X-ray

tube TXRF spectrometer (Wobicompact) that allows manually setting the incidence angle. The curve shape and broadening at the maximum is comparable to that of the thin film sample. On this basis, the angle position yielding the maximum intensity is selected as the best condition to test precision. Sample and hardware contributions to precision are evaluated, revealing that angle positioning and sample homogeneity are the most critical parameters, contributing net intensity uncertainties well below 10%.

Mono- and multi-elemental Pb loaded reference materials are measured to build the calibration curve. Based on various statistical tests, analytical parameters such as linear calibration range, limits of detection, and limits of quantification are determined for two datasets with different measurement times. The linear regression models include all the samples with high significance without issues related to matrix effects. Some improvements may be done to lower LODs and LOQs of the highest lifetime dataset that did not satisfy the performance requirements for environmental monitoring.

The versatility of the SMART STORE® approach for filter sample preparation, even though it significantly affects the intensity (mainly because of the absorption by the plastic), makes direct GIXRF analysis an alternative to other analytical techniques. Further studies will be dedicated to the assessment of the analytical performance and validation of this new approach using field test samples.

#### Declaration of Competing Interest

The authors declare that they have no known competing financial interests or personal relationships that could have appeared to influence the work reported in this paper.

#### Acknowledgement

The corresponding author personally likes to thank Angelo Borgese for his crucial contribution during data analysis; Diane Eichert, Thomas Hase and Giacomo Siviero for the insightful discussions on this paper topic.

This article/publication is based upon work from COST Action CA18130 European Network for Chemical Elemental Analysis by Total Reflection X-Ray Fluorescence ENFORCE TXRF, supported by COST (European Cooperation in Science and Technology).

#### References

- [1] B.R. Larsen, S. Gilardoni, K. Stenström, J. Niedzialek, J. Jimenez, C.A. Belis, Sources for PM air pollution in the Po Plain, Italy: II. Probabilistic uncertainty characterization and sensitivity analysis of secondary and primary sources, *Atmos. Environ.* 50 (2012) 203–213, <https://doi.org/10.1016/j.atmosenv.2011.12.038>.
- [2] A. Kholdebarin, A. Biati, F. Moattar, S.M. Shariat, Outdoor PM10 source apportionment in metropolitan cities—a case study, *Environ. Monit. Assess.* 187 (2015), <https://doi.org/10.1007/s10661-015-4294-z>.
- [3] F. Goodarzi, F.E. Huggins, H. Sanei, Assessment of elements, speciation of As, Cr, Ni and emitted Hg for a Canadian power plant burning bituminous coal, *Int. J. Coal Geol.* 74 (2008) 1–12, <https://doi.org/10.1016/j.coal.2007.09.002>.
- [4] E. Communities, Ambient air pollution by AS, CD and NI compounds. Position Paper, 2000 <http://europa.eu.int/comm/environment/pubs/home.htm> (accessed February 7, 2020).
- [5] B.J. Lee, B. Kim, K. Lee, Air pollution exposure and cardiovascular disease, *Toxicol. Res.* 30 (2014) 71–75, <https://doi.org/10.5487/TR.2014.30.2.071>.
- [6] L. Borgese, A. Zacco, S. Pal, E. Bontempi, R. Lucchini, N. Zimmerman, L.E. Depero, A new non-destructive method for chemical analysis of particulate matter filters: the case of manganese air pollution in Vallecarnonica (Italy), *Talanta.* 84 (2011) 192–198, <https://doi.org/10.1016/j.talanta.2010.12.048>.
- [7] Particulate Matter (PM) Pollution | US EPA, <https://www.epa.gov/pm-pollution>, (2017) (accessed February 7, 2020).
- [8] California Air Resources Board, Inhalable Particulate Matter and Health (PM2.5 and PM10), <https://ww2.arb.ca.gov/resources/inhalable-particulate-matter-and-health>, (2020) (accessed February 7, 2020).
- [9] Science for Environment Policy, Composition of Particulate Matter Influences its Long-term Health Effects, (2015), <https://doi.org/10.1016/j.envint.2015.05.00>.
- [10] F.D. Pope, M. Gatari, D. Ng&apos;ang&apos;a, A. Poynter, R. Blake, Airborne particulate matter monitoring in Kenya using calibrated low-cost sensors, *Atmos. Chem. Phys.* 18 (2018) 15403–15418, <https://doi.org/10.5194/acp-18-15403-2018>.
- [11] T.M. Peters, D. Ott, P.T. O'Shaughnessy, Comparison of the Grimm 1.108 and 1.109 portable aerosol spectrometer to the TSI 3321 aerodynamic particle sizer for dry particles, *Ann. Occup. Hyg.* 50 (2006) 843–850, <https://doi.org/10.1093/annhyg/mel067>.
- [12] A.M. Taiwo, D.C.S. Beddows, Z. Shi, R.M. Harrison, Mass and number size distributions of particulate matter components: comparison of an industrial site and an urban background site, *Sci. Total Environ.* 475 (2014) 29–38, <https://doi.org/10.1016/j.scitotenv.2013.12.076>.
- [13] F. Bilo, S. Moscoso, L. Borgese, M.V. Delbarba, A. Zacco, A. Bosio, S. Federici, M. Guarienti, M. Presta, E. Bontempi, L.E. Depero, Total reflection X-ray fluorescence spectroscopy to study Pb and Zn accumulation in zebrafish embryos, *X-Ray Spectrom.* 44 (2015) 124–128, <https://doi.org/10.1002/xrs.2588>.
- [14] L. Borgese, A. Zacco, E. Bontempi, P. Colombi, R. Bertuzzi, E. Ferretti, S. Tenini, L.E. Depero, Total reflection of x-ray fluorescence (TXRF): a mature technique for environmental chemical nanoscale metrology, *Meas. Sci. Technol.* 20 (2009), <https://doi.org/10.1088/0957-0233/20/8/084027>.
- [15] E. Bontempi, A. Zacco, D. Benedetti, L. Borgese, P. Colombi, H. Stosnach, G. Finzi, P. Apostoli, P. Buttini, L.E. Depero, Total reflection X-ray fluorescence (TXRF) for direct analysis of aerosol particle samples, *Environ. Technol.* 31 (2010) 467–477, <https://doi.org/10.1080/09593330903513260>.
- [16] R. Lucchini, S. Borghesi, G. Parrinello, High prevalence of parkinsonian disorders associated to manganese exposure in the vicinities of ferroalloy industries, *Am. J. Ind. Med.* 50 (2007) 788–800, <https://doi.org/10.1002/ajim.20494>.
- [17] M.J. Gatari, J. Boman, D.M. Maina, Inorganic element concentrations in near surface aerosols sampled on the northwest slopes of Mount Kenya, *Atmos. Environ.* 35 (2001) 6015–6019, [https://doi.org/10.1016/S1352-2310\(01\)00393-4](https://doi.org/10.1016/S1352-2310(01)00393-4).
- [18] J. Boman, M.J. Gatari, A. Wagner, M.I. Hossain, Elemental characterization of aerosols in urban and rural locations in Bangladesh, *X-Ray Spectrom.* 34 (2005) 460–467, <https://doi.org/10.1002/xrs.864>.
- [19] W.C. Hinds, *Aerosol Technology: Properties, 2nd ed.*, Wiley, 1999, <https://www.wiley.com/en-us/Aerosol+Technology%3A+Properties%2C+Behavior%2C+and+Measurement+of+Airborne+Particles%2C+2nd+Edition-p-9780471194101> (accessed February 7, 2020).
- [20] British Standards Institution, *Air Quality : Determination of the PM10 Fraction of Suspended Particulate Matter : Reference Method and field test Procedure to Demonstrate Reference Equivalence of Measurement Methods*, British Standards Institution, 1999.
- [21] ISO/TC 146/SC3, ISO - ISO 9855, Ambient air — Determination of the Particulate lead Content of Aerosols Collected on Filters — Atomic Absorption Spectrometric Method (1993) 7, <https://www.iso.org/standard/17734.html>, (1993) (accessed February 7, 2020).
- [22] Directive 2004/107/EC, The European Parliament and of the Council-Relating to Arsenic, Cadmium, Mercury, Nickel and Polycyclic Aromatic Hydrocarbons in Ambient Air, <https://eur-lex.europa.eu/LexUriServ/LexUriServ.do?uri=OJ:L:2005:023:0003:0016:EN:PDF>, (2004).
- [23] Directive 2008/50/EC, Air quality — European environment agency, Off. J. Eur. Union (2008), <https://www.eea.europa.eu/policy-documents/directive-2008-50-ec-of> (accessed February 7, 2020).
- [24] X.J. Yang, P. Wan, R. Foley, Effect of sample digestion, air filter contamination, and post-adsorption on the analysis of trace elements in air particulate matter, *Clean - Soil, Air, Water*, 40 2012, pp. 1217–1221, <https://doi.org/10.1002/clen.201100134>.
- [25] C.F. Wang, J.Y. Yang, C.H. Ke, Multi-element analysis of airborne particulate matter by various spectrometric methods after microwave digestion, *Anal. Chim. Acta* 320 (1996) 207–216, [https://doi.org/10.1016/0003-2670\(95\)00534-X](https://doi.org/10.1016/0003-2670(95)00534-X).
- [26] S. Yatkin, M. Gerboles, A. Borowiak, G. Tanet, V. Pedroni, R. Passarella, F. Lagler, Evaluation of EDXRF for the Determination of Elements in PM10 Filters, (2011), <https://doi.org/10.2788/87284>.
- [27] S. Yatkin, M. Gerboles, A. Borowiak, Evaluation of standardless EDXRF analysis for the determination of elements on PM 10 loaded filters, *Atmos. Environ.* 54 (2012) 568–582, <https://doi.org/10.1016/j.atmosenv.2012.02.062>.
- [28] I. De La Calle, N. Cabaleiro, V. Romero, I. Lavilla, C. Bendicho, Sample pretreatment strategies for total reflection X-ray fluorescence analysis: a tutorial review, *Spectrochim. Acta - Part B At. Spectrosc.* 90 (2013) 23–54, <https://doi.org/10.1016/j.sab.2013.10.001>.
- [29] EPA/625/R-96/010a, EPA Compendium of Methods for the Determination of Inorganic Compounds in Ambient Air, <https://www3.epa.gov/ttnamti1/files/ambient/inorganic/iocompen.pdf>, (1999) (accessed February 7, 2020).
- [30] R.M. Rousseau, J.P. Willis, A.R. Duncan, Practical XRF calibration procedures for major and trace elements, *X-Ray Spectrom.* 25 (1996) 179–189, [https://doi.org/10.1002/\(SICI\)1097-4539\(199607\)25:4<179::AID-XRS162>3.0.CO;2-Y](https://doi.org/10.1002/(SICI)1097-4539(199607)25:4<179::AID-XRS162>3.0.CO;2-Y).
- [31] S. Yatkin, K. Trzepla, W.H. White, N. Paily Hyslop, Generation of multi-element reference materials on PTFE filters mimicking ambient aerosol characteristics, *Atmos. Environ.* 189 (2018) 41–49, <https://doi.org/10.1016/j.atmosenv.2018.06.034>.
- [32] N.P. Hyslop, K. Trzepla, S. Yatkin, W.H. White, T. Ancelet, P. Davy, O. Butler, M. Gerboles, S. Kohl, A. McWilliams, L. Saucedo, M. Van Der Haar, A. Jonkers, An inter-laboratory evaluation of new multi-element reference materials for atmospheric particulate matter measurements, *Aerosol Sci. Technol.* 53 (2019) 771–782, <https://doi.org/10.1080/02786826.2019.1606413>.
- [33] S. Yatkin, H.S. Amin, K. Trzepla, A.M. Dillner, Preparation of lead (Pb) X-ray fluorescence reference materials for the EPA Pb monitoring program and the IMPROVE network using an aerosol deposition method, *Aerosol Sci. Technol.* 50 (2016) 309–320, <https://doi.org/10.1080/02786826.2016.1150956>.
- [34] L. Borgese, R. Dalipi, A. Riboldi, F. Bilo, A. Zacco, S. Federici, M. Bettinelli,

- E. Bontempi, L.E. Depero, Comprehensive approach to the validation of the standard method for total reflection X-ray fluorescence analysis of water, *Talanta*. 181 (2018) 165–171, <https://doi.org/10.1016/j.talanta.2017.12.087>.
- [35] ISO/TC 201/SC10, ISO - ISO 20289:2018 - Surface Chemical Analysis — Total Reflection X-ray Fluorescence Analysis of Water, 19 (2018) <https://www.iso.org/standard/67511.html> (accessed February 7, 2020).
- [36] L. Borgese, F. Bilo, S. Federici, E. Margui, T. Hase, Y. Huang, B. Beckhoff, L.E. Depero, Summary of ISO standard 20289: Total reflection X-ray fluorescence analysis of water, *Surf. Interface Anal.* (2019) 1–5, <https://doi.org/10.1002/sia.6720>.
- [37] R. Klockenkämper, A. von Bohlen, *Total-Reflection X-Ray Fluorescence Analysis and Related Methods*, 2nd ed., Wiley Blackwell, 2015, <https://doi.org/10.1002/9781118985953>.
- [38] E. Marguí, J.C. Tapias, A. Casas, M. Hidalgo, I. Queralt, Analysis of inlet and outlet industrial wastewater effluents by means of benchtop total reflection X-ray fluorescence spectrometry, *Chemosphere* 80 (2010) 263–270, <https://doi.org/10.1016/j.chemosphere.2010.04.027>.
- [39] H. Stosnach, Environmental trace-element analysis using a benchtop total reflection X-ray fluorescence spectrometer, *Anal. Sci.* 21 (2005) 873–876, <https://doi.org/10.2116/analsci.21.873>.
- [40] A. Shulyumova, A. Maltsev, N. Umarova, Multivariate calibration in TXRF analysis of water, *X-Ray Spectrom.* 47 (2018) 396–404, <https://doi.org/10.1002/xrs.2958>.
- [41] F. Bilo, L. Borgese, R. Dalipi, A. Zacco, S. Federici, M. Masperi, P. Leonesio, E. Bontempi, L. Depero, Elemental analysis of tree leaves by total reflection X-ray fluorescence: new approaches for air quality monitoring, *Chemosphere* 178 (2017) 504–512, <https://doi.org/10.1016/j.chemosphere.2017.03.090>.
- [42] M. Mages, M. Óvári, W.V. Tümling, K. Kröpfel, Biofilms as bio-indicator for polluted waters?: Total reflection X-ray fluorescence analysis of biofilms of the Tisza river (Hungary), *Anal. Bioanal. Chem.* 378 (2004) 1095–1101, <https://doi.org/10.1007/s00216-003-2291-5>.
- [43] A. Wagner, J. Boman, Biomonitoring of trace elements in muscle and liver tissue of freshwater fish, *Spectrochim. Acta - Part B At. Spectrosc.* 2003, pp. 2215–2226, <https://doi.org/10.1016/j.sab.2003.05.003>.
- [44] F. Bilo, A.Z. Laura Borgese, P. Lazo, C. Zoani, G. Zappa, E. Bontempi, L.E. Depero, Total reflection X-ray fluorescence spectroscopy to evaluate heavy metals accumulation in legumes, *J. Anal. Bioanal. Tech.* 7 (2016), <https://doi.org/10.4172/2155-9872.1000292>.
- [45] B. Markert, U. Reus, U. Herpin, The application of TXRF in instrumental multi-element analysis of plants, demonstrated with species of moss, *Sci. Total Environ.* 152 (1994) 213–220, [https://doi.org/10.1016/0048-9697\(94\)90312-3](https://doi.org/10.1016/0048-9697(94)90312-3).
- [46] K. Turnau, B. Ostachowicz, G. Wojtczak, T. Anielska, Ł. Sobczyk, Metal uptake by xerothermic plants introduced into Zn-Pb industrial wastes, *Plant Soil* 337 (2010) 299–311, <https://doi.org/10.1007/s11104-010-0527-7>.
- [47] L.M. Marcó, E.A. Hernández-Caraballo, Direct analysis of biological samples by total reflection X-ray fluorescence, *Spectrochim. Acta - Part B At. Spectrosc.* 2004, pp. 1077–1090, <https://doi.org/10.1016/j.sab.2004.05.017>.
- [48] G. Mankovskii, A. Pejović-Milić, Total reflection X-ray fluorescence based quantification of gold nanoparticles in cancer cells, *J. Anal. At. Spectrom.* 33 (2018) 395–403, <https://doi.org/10.1039/c7ja00332c>.
- [49] E. Marguí, R. Dalipi, L. Borgese, L.E. Depero, I. Queralt, Possibilities and drawbacks of total reflection X-ray fluorescence spectrometry as a fast, simple and cost-effective technique for multielement analyses of cosmetics, *Anal. Chim. Acta* 1075 (2019) 27–37, <https://doi.org/10.1016/j.aca.2019.05.005>.
- [50] E. Dasilva, A.M. David, A. Pejović-Milić, The quantification of total lead in lipstick specimens by total reflection X-ray fluorescence spectrometry, *X-Ray Spectrom.* 44 (2015) 451–457, <https://doi.org/10.1002/xrs.2629>.
- [51] B.J. Shaw, D.J. Semin, M.E. Rider, M.R. Beebe, Applicability of total reflection X-ray fluorescence (TXRF) as a screening platform for pharmaceutical inorganic impurity analysis, *J. Pharm. Biomed. Anal.* 63 (2012) 151–159, <https://doi.org/10.1016/j.jpba.2012.01.037>.
- [52] M. Wagner, P. Rostam-Khani, A. Wittershagen, C. Rittmeyer, B.O. Kolbesen, H. Hoffmann, Trace element determination in drugs by total-reflection X-ray fluorescence spectrometry, *Spectrochim. Acta - Part B At. Spectrosc.* 52 (1997) 961–965, [https://doi.org/10.1016/S0584-8547\(96\)01624-2](https://doi.org/10.1016/S0584-8547(96)01624-2).
- [53] F.J. Antosz, Y. Xiang, A.R. Diaz, A.J. Jensen, The use of total reflectance X-ray fluorescence (TXRF) for the determination of metals in the pharmaceutical industry, *J. Pharm. Biomed. Anal.* 62 (2012) 17–22, <https://doi.org/10.1016/j.jpba.2011.12.020>.
- [54] L. Borgese, F. Bilo, R. Dalipi, E. Bontempi, L.E. Depero, Total reflection X-ray fluorescence as a tool for food screening, *Spectrochim. Acta - Part B At. Spectrosc.* 113 (2015) 1–15, <https://doi.org/10.1016/j.sab.2015.08.001>.
- [55] X. Gruber, P. Kregsamer, P. Wobrauschek, C. Strel, Total-reflection X-ray fluorescence analysis of Austrian wine, *Spectrochim. Acta - Part B At. Spectrosc.* 61 (2006) 1214–1218, <https://doi.org/10.1016/j.sab.2006.08.006>.
- [56] A.A. Shaltout, E.S. Abdel-Hameed, F. Bilo, L. Borgese, L.E. Depero, Direct analysis of essential oils by means of TXRF spectrometry, *X-Ray Spectrom.* (2019), <https://doi.org/10.1002/xrs.3131>.
- [57] J. Prost, P. Wobrauschek, C. Strel, Quantitative total reflection X-ray fluorescence analysis of directly collected aerosol samples, *X-Ray Spectrom.* 46 (2017) 454–460, <https://doi.org/10.1002/xrs.2752>.
- [58] L. Borgese, M. Salmistraro, A. Gianoncelli, A. Zacco, R. Lucchini, N. Zimmerman, L. Pisani, G. Siviero, L.E. Depero, E. Bontempi, Airborne particulate matter (PM) filter analysis and modeling by total reflection X-ray fluorescence (TXRF) and X-ray standing wave (XSW), *Talanta*. 89 (2012) 99–104, <https://doi.org/10.1016/j.talanta.2011.11.073>.
- [59] F. Bilo, L. Borgese, A. Wambui, A. Assi, A. Zacco, S. Federici, D.M. Eichert, K. Tsuji, R.G. Lucchini, D. Placidi, E. Bontempi, L.E. Depero, Comparison of multiple X-ray fluorescence techniques for elemental analysis of particulate matter collected on air filters, *J. Aerosol Sci.* 122 (2018) 1–10, <https://doi.org/10.1016/j.jaerosci.2018.05.003>.
- [60] F. Bilo, L. Borgese, J. Prost, M. Rauwolf, A. Turyanskaya, P. Wobrauschek, P. Kregsamer, C. Strel, U. Pazzaglia, L.E. Depero, Atomic layer deposition to prevent metal transfer from implants: an X-ray fluorescence study, *Appl. Surf. Sci.* 359 (2015) 215–220, <https://doi.org/10.1016/j.apsusc.2015.09.248>.
- [61] P. Colombi, P. Bergese, E. Bontempi, L. Borgese, S. Federici, S.S. Keller, A. Boisen, L.E. Depero, Sensitive determination of the Young's modulus of thin films by polymeric microcantilevers, *Meas. Sci. Technol.* 24 (2013) 125603 (7pp), <https://doi.org/10.1088/0957-0233/24/12/125603>.
- [62] L. Borgese, F. Bilo, A. Zacco, E. Bontempi, M. Pasquali, S. Federici, J. Prost, M. Rauwolf, A. Turyanskaya, C. Strel, P. Kregsamer, P. Wobrauschek, L.E. Depero, ALD to prevent metal transfer from implants, *ECS Trans.*, Electrochemical Society Inc, 2016, pp. 167–175, <https://doi.org/10.1149/07506.0167ecst>.
- [63] L. Borgese, E. Bontempi, M. Gelfi, L.E. Depero, P. Goudeau, G. Geandier, D. Thiaudire, Microstructure and elastic properties of atomic layer deposited TiO<sub>2</sub> anatase thin films, *Acta Mater.* 59 (2011) 2891–2900, <https://doi.org/10.1016/j.actamat.2011.01.032>.
- [64] D. Ingerle, G. Pepponi, F. Meirer, P. Wobrauschek, C. Strel, JGIXA - a software package for the calculation and fitting of grazing incidence X-ray fluorescence and X-ray reflectivity data for the characterization of nanometer-layers and ultra-shallow-implants, *Spectrochim. Acta - Part B At. Spectrosc.* 118 (2016) 20–28, <https://doi.org/10.1016/j.sab.2016.02.010>.
- [65] D.K.G. De Boer, W.W. Van Den Hoogenhof, Total reflection X-ray fluorescence of single and multiple thin-layer samples, *Spectrochim. Acta Part B At. Spectrosc.* 46 (1991) 1323–1331, [https://doi.org/10.1016/0584-8547\(91\)80181-2](https://doi.org/10.1016/0584-8547(91)80181-2).